JOINT INSTITUTE FOR NUCLEAR RESEARCH

2004-199

M. G. Itkis

FLEROV LABORATORY OF NUCLEAR REACTIONS

RESEARCH ACTIVITIES IN 2004

Report to the 97th Session
of the JINR Scientific Council
January 20–21, 2005

Dubna 2004

M. G. Itkis

FLEROV LABORATORY OF NUCLEAR REACTIONS

RESEARCH ACTIVITIES IN 2004

Report to the 97th Session
of the JINR Scientific Council
January 20–21, 2005

Dubna 2004

In 2004, the FLNR scientific program on heavy ion physics included experiments on the synthesis of heavy and exotic nuclei using ion beams of stable and radioactive isotopes and studies of nuclear reactions, acceleration technology, heavy ion interaction with matter, and applied research. These lines of investigations were represented in fifteen laboratory and all-institute projects:

- Synthesis of new nuclei and study of nuclear properties and heavy ion reaction mechanisms (9 projects);
- Radiation effects and modification of materials, radioanalytical and radioisotopic investigations using the FLNR accelerators (5 projects);
- Development of the FLNR cyclotron complex for producing intense beams of accelerated ions of stable and radioactive isotopes (2 projects);
- Development of the U400+U400M+MT25 cyclotron-microtron complex for the production of radioactive ion beams (the DRIBs project).

In 2004, the operation time of the U400 and U400M FLNR cyclotrons was nearly 8000 hours, which is in accordance with the plan. Due to this, new experiments in low and medium energy ranges were possible.

Synthesis of new elements

Employing the Dubna Gas-filled Recoil Separator the dependence of the production cross sections of the isotopes $^{286-288}114$ on the excitation energy of the compound nucleus $^{290}114$ at four energies of ^{48}Ca projectiles has been studied (see Fig. 1). The properties of $^{286-288}114$ and their α-decay descendants coincide in full with those determined previously in cross bombardments reactions $^{244}Pu(^{48}Ca,4\text{-}5n)^{287,288}114$, $^{245}Cm(^{48}Ca,2\text{-}3n)^{290,291}116 \xrightarrow{\alpha} {}^{286,287}114$ and $^{249}Cf(^{48}Ca,3n)^{294}118 \xrightarrow{\alpha} {}^{290}116 \xrightarrow{\alpha} {}^{286}114$ [1].

The even-odd isotope $^{287}114$ undergoes mostly sequential α-α-SF decay with a typical total decay time of about 2-20 s. The total decay time is most strongly influenced by the relatively long-lived daughter nuclide $^{283}112$. The SF nuclide $^{279}110$ undergoes α-decay with a probability of about 10% which end in spontaneous fission of ^{271}Sg and ^{267}Rf. Their long lifetimes are caused by the influence of the deformed shells at Z=108 and at N=162.

During December 2003 through February 2004 excitation function of evaporation of 3 and 4 neutrons in the reaction $^{238}U+^{48}Ca$ [2] were measured at three energies of ^{48}Ca (Fig. 1).

The investigation of reaction $^{233}U+^{48}Ca$ opened for the first time a possibility of applying the method of genetic correlations to identify products the reaction of ^{48}Ca with actinide target. Here the evaporation of 2 to 4 neutrons leads to the known nuclide $^{277}112$ and to $^{278,279}112$, whose α-decays lead to the known ^{270}Hs and ^{263}Rf. However, the calculated fission barriers of the nuclei to be produced in this reaction are considerably lower than those of the heavier ones, which should result in a corresponding decrease of production cross sections. Indeed, the reaction cross section appeared to be below 0.6 pb, that gives a support to the hypothesis concerning the influence of stability (or fission barriers) of nuclei on the cross section of their production.

In April-May 2004 the irradiation of ^{248}Cm by ^{48}Ca ions was performed. In 2000- 2001 the first three atoms of element 116, $^{293}116$, were synthesized in this reaction. In the latter experiment higher energy of ^{48}Ca was used that resulted in a considerable increase of the reaction cross sections (Fig. 1). Six decays of the new even-even isotope $^{292}116$ (E_α=10.66 MeV, T_α=18 ms) were observed.

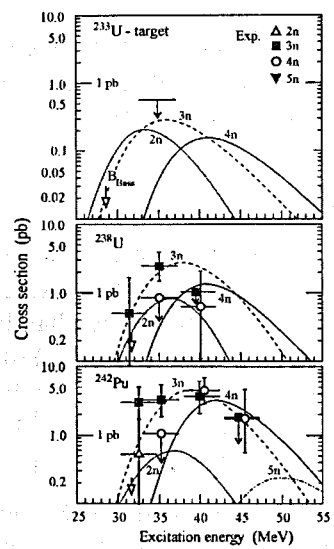

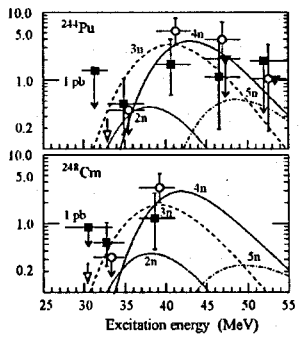

Fig. 1. Excitation functions for the 2n (Δ), 3n (■), 4n (○)and 5n (▼) evaporation channels from the complete-fusion reactions $^{233,238}U$, $^{242,244}Pu$, $^{248}Cm+^{48}Ca$.

The observed decay properties of the four isotopes of element 114 with masses 286-289 provide a consistent mass-identification for all of the heavier even-Z nuclei, in particular, the four isotopes of element 116 with masses 290-293 that were synthesized earlier in the reactions $^{245,248}Cm+^{48}Ca$, and also the isotope of element 118 with A=294 observed as an α-α-SF chain in the reaction $^{249}Cf+^{48}Ca$. They define also the masses of neutron-rich nuclei with Z=104-108 that appear in the decay chains of the mother nucleus $^{287}114$.

As a whole, they give a consistent pattern of decay of the 18 even-Z neutron-rich nuclides with Z=104-118 and N=163-177.

The decay properties of nuclei in the decay chain $^{290}116 \xrightarrow{\alpha} {}^{286}114(\alpha/SF) \xrightarrow{\alpha} {}^{282}112(SF)$, synthesized individually in the three reactions ^{245}Cm, ^{242}Pu, $^{238}U+^{48}Ca$, coincide well with those measured for the descendant nuclei of the heavy even-even nuclide $^{294}118$ produced in the reaction $^{249}Cf(^{48}Ca,3n)^{294}118$.

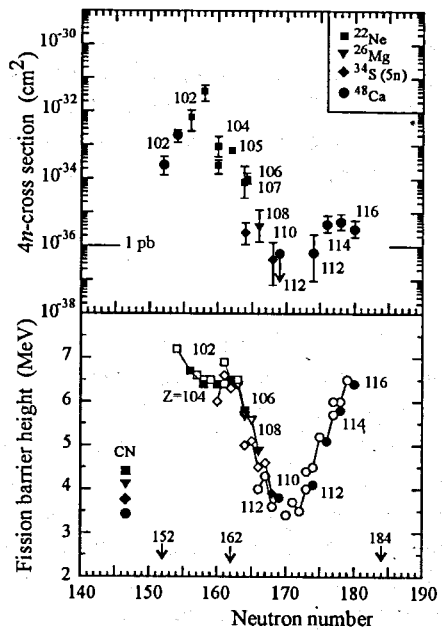

Fig. 2. Comparison of hot fusion cross-sections for the production of Z≥102 nuclides using a variety of heavy-ion beams (top panel). The fission barrier heights as a function of neutron number (bottom panel). Solid symbols correspond to the number of neutrons in compound nuclei formed in different reactions.

All the observed α-decay sequences end in SF characterized by a high TKE of the fragments. For superheavy nuclei with Z≥110, the value of TKE increases with Z following the dependence of TKE vs. $Z^2/A^{1/3}$ expected for asymmetric fission. Spontaneous fission of the nuclei with Z=106 and N=165, as well as $^{267,268}Db$ (N=162, 163) with an abnormally high kinetic energy release is most probably associated with the symmetric fission decay mode.

The production cross sections in the complete fusion reactions with ^{48}Ca are determined by the survivability of nuclei and depend mostly on their fission barrier height. The expected increase of fission barrier heights on approaching the neutron shell at N=184 leads to an increase in the evaporation residue cross section; a conclusion supported by experimental data (see

Fig. 2). Thus, the effect of nuclear shells in the domain of superheavy elements results not only in substantially higher stability to various decay modes, but also in an increase of the production cross section for complete fusion reactions with ^{48}Ca projectiles. The observed 3-5 MeV upward shift of the maxima of the evaporation residue yields in the reactions of actinide nuclei with ^{48}Ca projectiles with respect to the calculated Coulomb barrier for spherical nuclei can be attributed to the selection of the entrance states associated with the orientation of the deformed target nuclei in collisions with ^{48}Ca.

The present experimental data on the production cross sections and decay properties of even-Z nuclides can be used for determining the conditions for synthesis and prediction of the decay properties of odd-Z nuclides. Our interpretation of the data of the experiments on the synthesis of element 115 in the reactions ^{243}Am(^{48}Ca,3-4n)^{288,287}115 [3] is in agreement with the results of the recent experiments.

Chemistry of transactinides

The recent discovery of the elements 115 and 113 in the reaction ^{48}Ca + ^{243}Am [3] was confirmed by an independent radiochemical experiment based on the identification of the long-lived decay product dubnium [4].

All of the new nuclides were synthesized in ^{48}Ca induced reactions employing physical techniques. Their identification is based on their radioactive decay properties and the reaction mechanism, in particular, on the characteristic dependence of the yield of neutron-evaporation products on the excitation energy of the compound nucleus. The chemical identification of isotopes could give the identity of the atomic numbers of nuclei and provide independent evidence for the discovery of a new element.

An isotope of element 115 with mass number 288 was synthesized[6] in the reaction ^{48}Ca+^{243}Am$\rightarrow$^{288}115+3n. It undergoes five sequential α-decays ($115 \xrightarrow{\alpha} 113 \xrightarrow{\alpha} 111 \xrightarrow{\alpha} 109 \xrightarrow{\alpha} 107 \xrightarrow{\alpha} 105 \xrightarrow{SF}$) ending with the spontaneous fission of ^{268}Db. The half-life of the spontaneously fissioning final nucleus ^{268}Db was estimated from the three observed events to be $T_{1/2}=16^{+19}_{-6}$ hours. For chemical identification, the element should be separated according to its group properties.

According to the atomic configuration in the ground state ([Rn]5d^{14}6p^{3}7s^{2}), Db should belong to the 5th group of the Periodic Table as a heavier homologue of Nb and Ta. Bearing in mind that the Z=105 isotope of

interest undergoes SF, we paid special attention to separating the group 5 elements from the actinides and, most importantly, from spontaneously fissioning isotopes of californium, ^{252}Cf ($T_{1/2}$=2.65 y, SF – 3.1%) and ^{254}Cf ($T_{1/2}$=60.5 d, SF – 99.7%). The separation from the actinides including Lr simultaneously answers the question if ^{268}Db undergoes an additional decay followed by spontaneous fission of ^{264}Lr.

The experiment was performed at the FLNR (JINR) U-400 cyclotron in June, 2004. The principal scheme of set-up for target irradiation is shown in Fig. 3.

The 32-cm^2 rotating target consisted of the enriched isotope ^{243}Am (99.9%) in the oxide form deposited onto 1.5-μm Ti foils to a thickness of 1.2 mg/cm^2 of ^{243}Am. The target was bombarded by ^{48}Ca ions with an energy corresponding to 247 MeV in the middle of the target with an average intensity of 5×10^{12} ions/s. The recoiling reaction products on leaving the target passed through a 12-mm collimator positioned 10 mm from the target, and were stopped in the 50-mm diameter copper catcher block. A total of eight similar experimental runs with duration between 20 to 45 hours were performed.

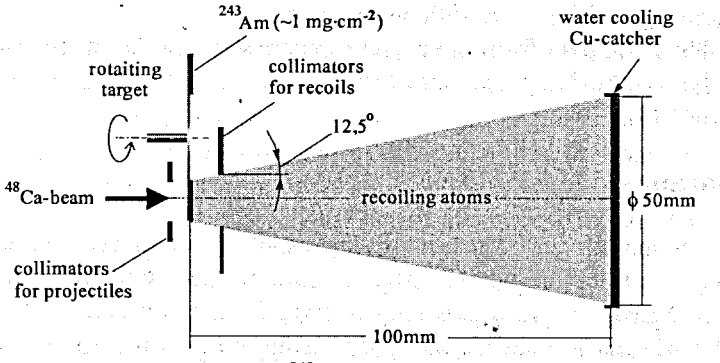

Fig. 3. The scheme of set-up for ^{243}Am target irradiation and collection of recoiling products.

The chemical procedure took 2 to 3 hours, starting from the end of irradiation until the beginning of detector measurements. For the registration of α-particles and spontaneous fission fragments the sample under study was placed between two semiconductor detectors which were positioned inside a neutron detector registering spontaneous fission neutrons. The efficiency of detecting fission fragments in the semiconductor detectors was about 90% and neutrons were detected with an average efficiency of about 40%. In the course of the 330-hour test run performed before the experiment no background SF events were detected.

During eight runs of irradiating the ^{243}Am target with ^{48}Ca ions (with a total beam dose of 3.4×10^{18}), we detected 15 spontaneous fission events. The measurements were carried out for a total of 957 hours.

The half-life of 32^{+11}_{-7} hours determined from the time distribution of SF events agrees with the half-life obtained in the physical experiment within statistical errors. The total kinetic energy of the fission fragments ($\overline{TKE}$) was about 235 MeV. This result also agrees with the data from the physical experiment ($\overline{TKE}$ ~225MeV). The average neutron multiplicity per fission was ν~4.2. Both parameters, i.e., the high $\overline{TKE}$ value and the high neutron multiplicity, give evidence for the fission of a rather heavy nuclide. For comparison, in the spontaneous fission of ^{248}Cm, $\overline{TKE}$ =181 MeV and ν=3.14 and in ^{252}Cf, $\overline{TKE}$ =185 MeV and ν=3.75.

From the yield of spontaneously fissioning nuclei, one can determine the cross section of the parent nucleus – element 115 – as an evaporation product from the reaction ^{243}Am+ ^{48}Ca. According to our data this formation cross section is about 4 pb. This agrees with the value (σ_{3n}~3 pb) measured in the experiments with the gas-filled separator.

Thus, the data from the present experiment are the independent evidence for the synthesis of element 115 as well as element 113 in the reaction ^{243}Am+^{48}Ca.

Separator "MASHA"

The manufactured separator was installed in a special testing room at the FLNR. Tests of the whole setup are running now both with the plasma ion source FEBIAD and a specially designed ECR ion source. In experiments with a plasma ion source the mass resolution Δm/m of $3\cdot10^{-4}$ was achieved for Kr, Xe and Hg isotopes (Fig. 4).

The setup MASHA surpass all known facilities both in efficiency of obtaining superheavy atoms and in extracting information on the their masses and decay characteristics. It also opens up new possibilities for the study of chemical properties of superheavy elements.

It should be noted that due to the high efficiency of the chemical separation of the reaction products and the possibility of employing relatively thick target layers, the yield of the isotopes of superheavy is about a factor of five higher than that obtained with kinematic separators. This will allow the use of MASHA in off-line mode for precise mass determination of ^{48}Ca+^{243}Am reaction products.

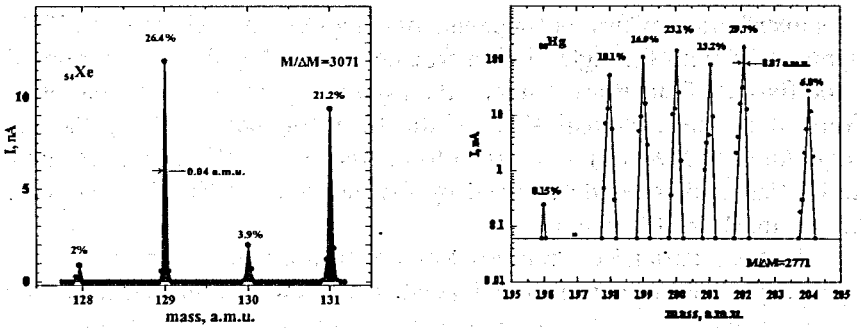

Fig. 4. Mass-spectra of ^{nat}Xe and ^{nat}Hg isotopes produced with MASHA separator.

First experiments with the use of this separator and the ^{48}Ca beam of the U400 cyclotron are scheduled for 2005.

Nuclear fission

The main task in 2004 was to carry out experiments aimed at understanding the dynamics of the process of formation and decay of superheavy nuclei with Z=116-122. The main attention was paid to the influence of the entrance channel, evolution of the compound nucleus shape, from the moment of its formation to the scission point, and the competition between different exit channels (fission, quasifission, formation of the evaporation residue). Measurements of the angular, mass and energy distributions of fission fragments allowed us to obtain information on the process of the compound nucleus fusion-fission as well as on the process of quasifission. The cross sections of these two processes were determined.

In 2004, the experimental data obtained in the study of mass-energy distributions of fission fragments and the excitation functions of superheavy nuclei with Z=102-122, formed in the reactions ^{26}Mg+^{248}Cm; ^{48}Ca+^{208}Pb, ^{232}Th, ^{238}U, ^{244}Pu, ^{248}Cm; ^{58}Fe+^{208}Pb,. ^{232}Th, ^{244}Pu, ^{248}Cm at energies close to or below the Coulomb barrier, were analyzed. A series of experiments was carried out at the Flerov Laboratory of Nuclear Reactions with the use of the double-arm time-of-flight spectrometer CORSET. As a result of the experiments, a strong manifestation of shell effects in the quasifission fragments of nuclei with Z=112-122 due to the influence of the shells with Z=28 and N=50 in the light fragment and those with Z=28 and N=126 in the heavy fragment was discovered.

As a result of the analysis of mass distributions (MD) of fragments of the superheavy nucleus (Z=102-122) fission, a decomposition of the fusion-fission and quasifission contributions was performed. It was found that the

mass distribution of fission fragments of compound nuclei with Z=112-122 is asymmetric, with the light fission fragment mass $M_L \approx 132$-134 a.m.u. Thus, in the fission of superheavy nuclei the asymmetry of mass distribution is determined by the spherical shell of the light fragment, i.e., by the doubly magic tin (Z=50, N=82), in contrast to the fission of actinide nuclei, in which the MD asymmetry is determined by the deformed shell of the heavy fragment with $M_H \approx 140$ a.m.u. [5].

The competition between processes of fusion-fission and quasifission of supeheavy nuclei was studied in dependence on the entrance reaction channel and the shell structures of colliding nuclei and formed compound nucleus. For the reactions with ^{48}Ca ions a systematization of relations between fusion and quasifission cross sections as a function of mass of the formed composite nucleus was made. It was found that the contribution of quasifission decreases greatly in the case of the reactions in which magic spherical nuclei were used as targets. For the superheavy nuclei ^{274}Hs and ^{256}No a phenomenon of the multi-modal fission was discovered at low excitation energies .

In the framework of the collaboration with the LNL (Legnaro, Italy) investigations of fission and evaporation residue formation cross sections were continued. Also, mass-energy and angular distributions of fission fragments of ^{192,202}Pb produced in the reactions ^{48}Ca +^{144,154}Sm were measured (Fig. 5) [6]. In the reaction with a strongly deformed target ^{154}Sm an asymmetric component was discovered in the mass distribution of fission fragments at energies close to or below the Coulomb barrier. The yield of this component increases with a decrease in the excitation energy. The angular distribution for this component is strongly asymmetric, which confirms the quasifission nature of the component. In the case of the spherical target ^{144}Sm the latter was not found.

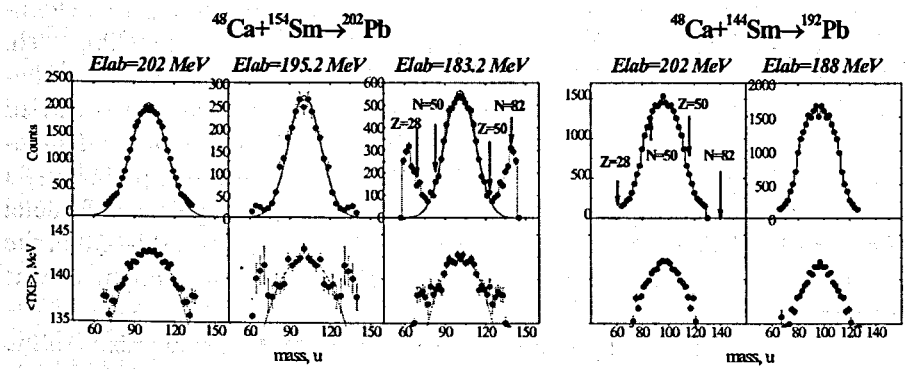

Fig 5. Fission fragment mass-energy distributions at different ^{48}Ca energies for ^{48}Ca + $^{144, 154}$Sm reactions.

Mass-angular distributions of fission and quasifission fragments were experimentally measured in reactions ^{44}Ca + ^{206}Pb → ^{250}No, ^{64}Ni +^{186}W → ^{250}No near the Coulomb barrier. A strong manifestation of the quasifission component was observed in the more symmetric reaction ^{64}Ni +^{186}W → ^{250}No as compared with ^{44}Ca + ^{206}Pb → ^{250}No (Fig. 6). From the analysis of the mass-energy distributions it follows that only a small part of the fragment yield (~25%) may be associated with the fusion-fission of the compound nucleus in the reaction ^{64}Ni +^{186}W, the quasifission process being the major decay channel, whereas for the reaction ^{44}Ca + ^{206}Pb about 70% of the total number of events can be attributed to the fission of the ^{250}No compound nucleus.

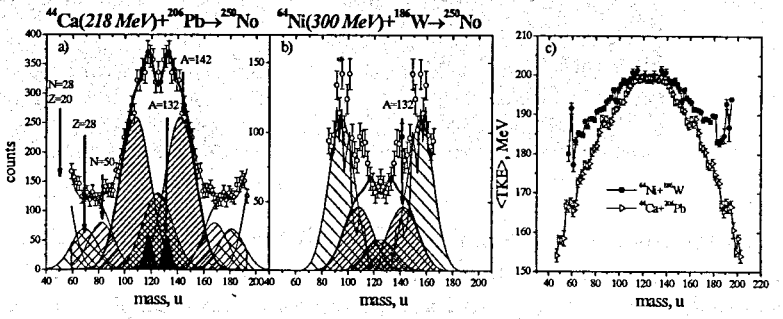

Fig. 6. Mass distributions for ^{44}Ca+^{206}Pb (a) and ^{64}Ni+^{186}W (b) reactions and average kinetic energies <TKE> as a function of fragment mass (c) for these reactions at the excitation energy of 30 MeV.

Separator VASSILISSA

A new detector system has been designed to measure decay properties of reaction products transported to the focal plane of the recoil separator VASSILISSA. It comprises a system of timing detectors based on microchannel plates, as well as silicon and germanium detectors optimized for detecting the arrival of the reaction products and correlating with any subsequent radioactive decays, involving emission of α-, β-particles, γ-rays, X-rays and fission fragments.

The aim of the project is to benefit from the radioactive actinide targets uniquely available at Dubna and from the very intense stable beams provided by the U400 cyclotron. It will be thus possible for the first time to study nuclei above Z=100 along an isotopic chain approaching N=162.

The recoil nuclei are implanted into the stop 16 strip detector. In the backward direction, 4 electron detectors were placed. The focal plane detector is surrounded with 7 Ge detectors (Fig. 7).

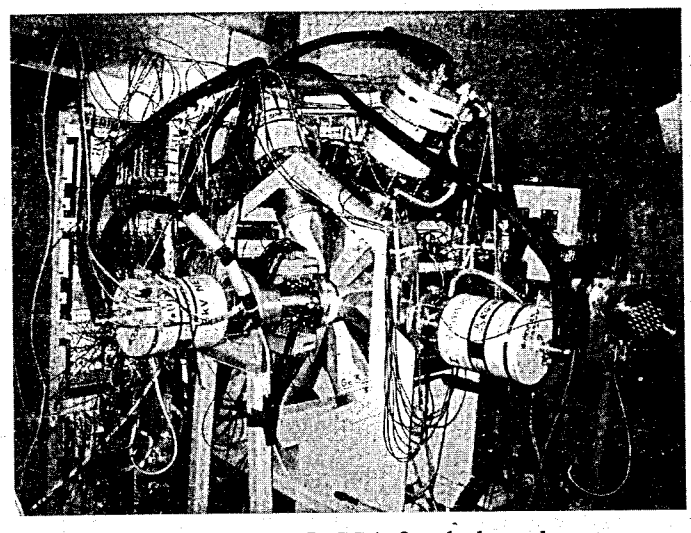

Fig. 7. General view of the VASSILISSA focal plane detector assembly.

To test the new detector together with electronic and data acquisition systems complete fusion reactions $^{48}Ca + {}^{164}Dy \rightarrow {}^{212}Rn^*$, $^{40}Ar + {}^{174}Yb \rightarrow {}^{214}Ra^*$ and $^{40}Ar + {}^{181}Ta \rightarrow {}^{221}Pa^*$ at excitation energies of compound nuclei corresponding to the deexcitation channels with the evaporation of 4 - 5 neutrons were studied.

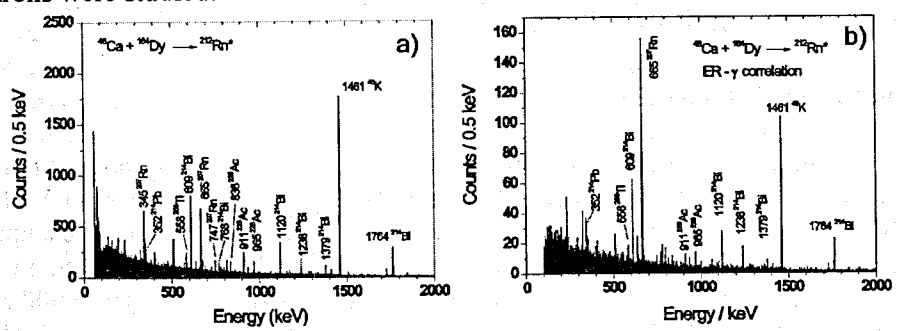

Fig. 8. An example of the recorded γ-spectra **a)** by one Ge detector with BGO anti-Compton cleaning and **b)** the same spectrum using ER - γ correlation analysis - for the reaction $^{48}Ca + {}^{164}Dy \rightarrow {}^{212}Rn^*$.

At a beam intensity of about 0.7 pμA the counting rate of scattered ions and other unwanted products at the focal plane detector was less than 50 Hz. The counting rate of background gamma's at this beam intensity in one Ge detector was about 1 kHz. With the use of anticoincidence with BGO anti-Compton shields this rate was reduced to 300 Hz. Fig. 8 illustrates the γ-

spectra recorded for the reaction $^{48}Ca + {}^{164}Dy \rightarrow {}^{212}Rn^*$. It is clearly seen how an ER - γ correlation analysis "cleans" the spectrum, γ transitions from the isomeric state of ^{207}Rn are well pronounced.

In the first full-scale experiment complete fusion reactions $^{48}Ca + {}^{207,208}Pb \rightarrow {}^{255,256}No^*$ and $^{48}Ca + {}^{209}Bi \rightarrow {}^{257}Lr^*$ were investigated. The decays of the isotopes $^{253,254,255}No$ and ^{255}Lr and their daughter products were studied. The data are now under analysis.

Fragment separator COMBAS

During 2004 year on the in-flight separator COMBAS, the number of experiments has been carried out devoted to the production of ^{13}B, ^{14}B, ^{15}B radioactive beams and the study of cluster structure of ^{11}B.

In reaction fragmentation of ^{18}O (35 AMeV) + ^{9}Be, the production rates of neutron-rich nuclei ^{13}B ($2*10^6$ 1/s), ^{14}B ($5*10^5$ 1/s), ^{15}B ($3*10^5$ 1/s) have been determined which can be used to study the cluster structure of these nuclei. The multi-detector system from 32 strips Si detectors has been commissioned and installed in the COMBAS focal plane to register the coincidences of $^{11-15}B$ breakup products. The multi-channel electronics system and the appropriate data acquisition system have been designed and built to satisfy the demand of multi-particle spectroscopy measurements. In the inelastic reaction ^{11}B (33 AMeV) + ^{12}C (0.28 mg/cm^2) → ($^{7}Li + {}^{4}He$) + $^{12}C^*$, the test $^{11}B^*$ breakup experiment have been performed. Now produced experimental data is processing and analyzing. Using the Quantum Molecular Dynamics (QMD) model (CHIMERA code), the simulations of velocity, isotopic and element distributions of fragmentation products induced in the reactions ^{18}O (35 AMeV) + ^{9}Be (^{181}Ta) were implemented and compared with experimental data [7].

High-resolution beam-line ACCULINNA

Earlier the observation of the ^{5}H ground state resonance produced in the reactions $^{6}He+{}^{1}H$ and $^{3}H+{}^{3}H$ reactions was reported. The two reactions gave similar values, 1.7 – 1.8 MeV for energy of the ^{5}H ground state resonance. However discrepancy remained in respect to the resonance width: surprising was the unexpectedly small width of this resonance maximum ($\Gamma_{obs} \leq 0.5$ MeV). This prompted the further study of this nucleus.

Experiments aimed at the ^{5}H nucleus production were carried out at triton beam energy of 58 MeV, in the t+t reaction in different kinematical con-

ditions. In the present study protons ejected in the reaction ^{3}H(t,p)^{5}H were detected in a range of θ_{lab}=173°–155°, corresponding, in CM system, to a very backward direction branch (see the detector array in Fig. 9).

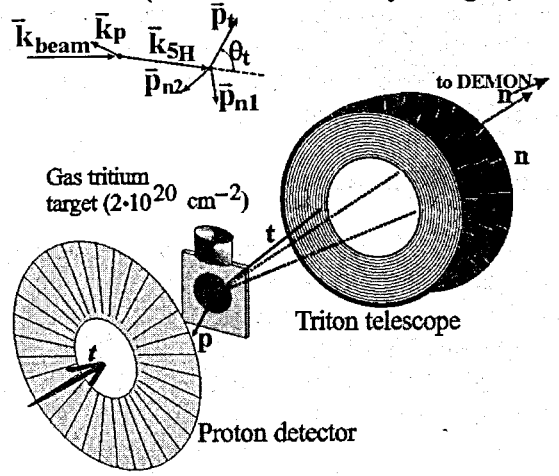

Fig. 9. ACCULINNA detector array.

Tritons and neutrons emitted at the ^{5}H decay were detected in coincidence with the protons. 49 DEMON modules installed in forward direction detected at least one decay neutron with a high efficiency. The detection of triple p-t-n coincidence uniquely identified the outgoing reaction channel making possible a complete kinematical reconstruction.

Data in the center-of-mass (CM) system of ^{5}H (t+2n) are shown by diamonds in Figs. 10, 11. The direction of the momentum transfer $\mathbf{k}_{beam}-\mathbf{k}_p$ occurring in the reaction ^{3}H (t,p)^{5}H was chosen as the Z axis. The ^{5}H missing mass spectrum is shown in Fig. 10. Fig. 11 shows the distribution of the ^{5}H decay energy between the relative motions in the t-nn and nn subsystems (presented in terms of the E_{nn}/E_{5H} ratio). It shows a narrow peak corresponding to a strong "dineutron" final state interaction.

The most striking result is the observation of a sharp oscillating picture in the triton angular distribution. Such correlations can be obtained only for very specific conditions. The bulk of the data observed in these experiments can be explained only by the assumption that the direct transfer of two neutrons (ΔL=2, ΔS=0) dominates in the ^{3}H (t,p)^{5}H reaction leading to the population of the broad, overlapping 3/2$^+$and 5/2$^+$ states in ^{5}H. According to theory prediction, one can consider these excited states as degenerate.

The following procedure for data analysis was employed. Correlations occurring at the ^{5}H decay are described as:

$$W = \sum_{JM,J'M'} \langle J'M'|\rho|JM\rangle A^*_{J'M'} A_{JM}$$

J, M are the total ^{5}H spin and its projection, A_{JM} are the decay amplitudes depending on the ^{5}H decay dynamics. $\langle$ J'M'|ρ|JM$\rangle$ is the density matrix, which describes the polarization of the ^{5}H states populated in the reaction and takes into account the mixing of the 3/2$^+$ and 5/2$^+$ states. The amplitudes A_{JM} were expanded over a limited set of hyperspherical harmonics (assumed to be the same for the 3/2+ and 5/2+ states) [8].

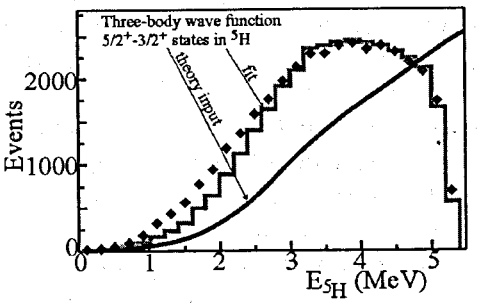

Fig. 10. Missing mass spectrum of ^{5}H.

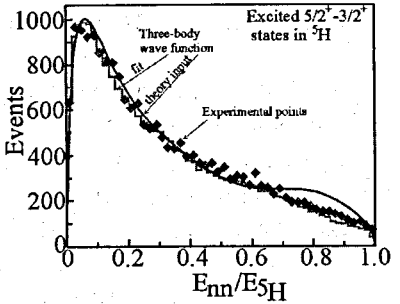

Fig. 11. Spectrum of relative energy for two neutrons.

Agreement obtained between the data and the MC results is excellent at E_{5H}>2.5 MeV. Below this energy, one could not achieve an agreement assuming the interference of only 3/2$^+$ and 5/2$^+$ states, one can reproduce the correlations obtained at E_{5H}<2.5 MeV by assuming the interference of the 1/2$^+$ ground state with the 3/2$^+$-5/2$^+$ doublet. This can be takens as an evidence for the population of the ^{5}H g.s. lying at about 2 MeV.

The missing mass spectrum of ^{5}H obtained in this work shows a broad structure above 2.5 MeV. The observed strong correlation pattern allows to identify unambiguously this structure as a mixture of the 3/2+ and 5/2$^+$ states. Such a correlation is a rare phenomenon for transfer reactions involving particles with nonzero spin and means that the 3/2$^+$ and 5/2$^+$ states are either almost degenerate or the reaction mechanism causes a very specific interference of these states.

Approach assuming the observation of a T=3/2 isobaric spin state in ^{5}He could provide useful information on the energy and width of the ^{5}H ground state resonance. Such an analog state in ^{5}He remained as yet unknown. In the present study the ^{2}H(^{6}He,^{3}He)^{5}H and ^{2}H(^{6}He,t)^{5}He reactions were explored, studied at a ^{6}He beam energy of 132 MeV, to observe the ground state in ^{5}H and the lowest T=3/2 state in ^{5}He, both having the $(1s)^3(1p)^3$ configuration. These reactions correspond to the pickups of either proton or neutron from

the α core of ^{6}He. The kinematics of these reactions is similar, and their relative yields are governed by the isospin selection rule.

Two telescopes were employed in the experiment aimed at this study. The first telescope detected reaction ejectives (^{3}He, t) emitted at lab angles 25±7 degrees, whereas the second telescope was used for decay particles emitted at 16±11 degrees. These were the tritons that appeared after the decay of ^{5}H and ^{3}He nuclei, tritons or deuterons which could originate from different ^{5}He decay modes.

In the case of the ^{2}H(^{6}He,^{3}He) reaction the data show a resonance at E_{obs}=2.2±0.4 MeV with a width of Γ_{obs}=2.5 MeV. It is conceivable to attribute the 2.2 MeV resonance to the ground state of ^{5}H.

Data obtained for the ^{2}H(^{6}He,t) reaction indicate that a resonance state in ^{5}He with isobaric spin T=3/2 located at an excitation energy E_{obs}=22.1±0.3 MeV and having a width Γ_{obs}=2.5±0.3 MeV was observed. It was found that this state showed up in the ^{5}He the three-body decay modes allowed for the T=3/2 state. The cross sections were estimated to be, respectively, 0.10±0.03mb/sr and 0.2±0.1 mb/sr for the ^{5}He→^{3}He+n+n and ^{5}He→t+p+n decay modes of the ^{5}He isobaric analog state.

Exotic decay modes. 4π-detector FOBOS

The major efforts of the FOBOS group during this year were concentrated on the study of a new type of nuclear transformation, namely collinear cluster tripartition (CCT) discovered earlier in our experiments at the FOBOS setup. The new experimental facility, the Modified Mini-FOBOS setup (MMF), was successfully put into operation. It was specially optimized for the investigation of the characteristics of the CCT decay channel of heavy nuclei, powered by the Transformable Neutron Skin (TNS) and equipped by the new electronic system for identification of events where two fragments hit one and the same detector in a short time interval. Two experiments were performed successfully with MMF setup during this year [9]. The analysis of experimental data is in progress. The data measured with the FOBOS spectrometer some years ago were reanalyzed employing the new mathematical formalism specially developed. Clear confirmation of the CCT was obtained for the decays of the ^{252}Cf (Fig. 12) and ^{248}Cm nuclei.

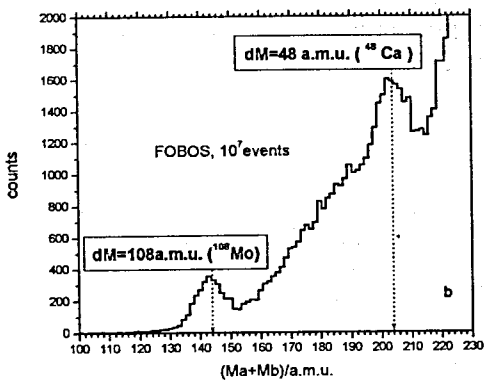

Fig. 12. Spectrum of the total mass of detected fission fragments of ^{252}Cf (sf).

Reactions induced by stable and radioactive ion beams of light elements

At the U400M cyclotron experiments were performed to measure the excitation functions of fusion reactions with the consequent evaporation of neutrons from compound nucleus ^{215}At, produced in reactions ^{208}Pb(^{7}Li,xn)$^{215\text{-}xn}$At and ^{209}Bi(^{6}He,xn)$^{215\text{-}xn}$At [10]. The excitation functions for the fission of the ^{215}At nucleus formed with both beams were also measured. The measurements were carried out in the projectile energy range 7-25 MeV/nucleon. In the case of the ^{7}Li beam excitation functions were obtained for the 3-9-neutron evaporation channels, whereas for the case of the ^{6}He beam – for the 4-8-neutron evaporation channels (Fig. 13). The ^{6}He beam was produced as a secondary beam in the interaction of a ^{7}Li beam with a beryllium target. The experiments were performed using the multi-detector setup MULTI.

The comparative analysis of the excitation functions for the two studied reactions ^{6}He+^{209}Bi and ^{7}Li+^{208}Pb showed that these functions are identical within the experimental errors for a broad range of excitation energy. This fact can serve as evidence that in the interaction of the weakly bound nuclei ^{7}Li and ^{6}He at energies above the Coulomb barrier no peculiarities of the entrance channel are manifested and the decay of the formed compound nucleus is determined solely by its properties. The study of the excitation functions of these reactions at energies close to the Coulomb barrier will be continued at the DRIBs complex.

Measurements were also carried out of the total reaction cross section σ_R for the ^{4,6}He+^{28}Si and ^{7}Li +^{28}Si reactions in the energy range 5-50 MeV/nucleon [11]. The experiments were done using the transmission method in a multi-layer semiconductor telescope. The use of thin Si detectors with thickness 20-300 μm made it possible to measure in detail the energy dependence of σ_R with an energy resolution $\delta E \sim 1$ MeV/nucleon.

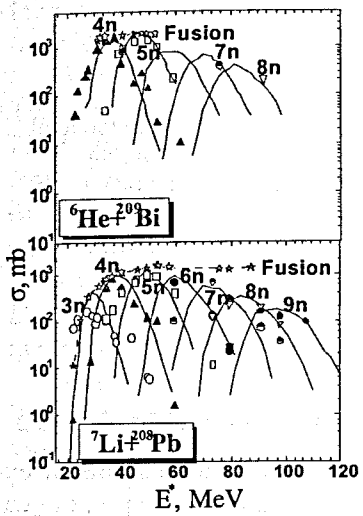

Fig. 13. Excitation functions for xn-evaporation channels and complete fusion in the ^{6}He+^{209}Bi and ^{7}Li+^{208}Pb reactions.

The analysis of the data revealed a peculiarity in the total reaction cross section for the ^{6}He+^{28}Si reaction in the energy range 10-20 MeV/nucleon, viz. the cross section exceeds the theoretical calculations by about 150-200 mb. This may be due to the manifestation of the single-particle interactions of neutrons, forming a halo, and the target protons.

Another series of experiments was dedicated to the investigation of the nuclear structure of fission fragments using the methods of resonance laser spectroscopy. A technique has been developed for measuring the quadrupole moments of the odd isotopes ^{93}Zr and ^{95}Zr. These isotopes were produced by chemical separation from a uranium target, which had been irradiated by brehmsstrahlung at the FLNR microtron. The samples, obtained in this way, were studied in the order to determine the quadrupole deformation of ^{93}Zr and ^{95}Zr. The analysis of the experimental data is in progress and will allow determining the change of deformation with increasing the neutron excess of the nuclei.

Theoretical and computational physics

Systematic analysis of reaction dynamics of super-heavy nucleus formation and decay at beam energies near the Coulomb barrier has been performed [12]. Three-dimensional potential energy surfaces in the space of "elongation-deformation-mass-asymmetry" have been calculated and used for analysis of SHE formation and quasi-fission processes within the model proposed earlier. Main attention was paid to the orientation effect in collisions of statically deformed nuclei and its influence on formation of heavy CN. It was shown that tip collisions lead the system mainly to the quasi-fission channels, whereas side collisions are more preferable for formation of CN. This effect shifts still more the EvR excitation functions of SHE formation in asymmetric fusion reactions induced by ^{48}Ca to higher energies close to the Coulomb barriers of the side configurations.

Dynamical calculations were carried out using the Langevin equations combined with the statistical model for pre-scission neutron evaporation. Several projectile-target combinations leading to formation of super-heavy nuclei have been studied within the model [13]. Mass distribution of fission and quasi-fission fragments was calculated and a reasonable agreement with experimental data was obtained. Pre-scission neutron multiplicity was also calculated and compared with experimental data. Two components have been found in neutron distributions which may be attributed to the quasi-fission and regular fusion-fission processes. This fact could be very important for further study of dynamical evolution of heavy nuclear systems.

A new mechanism – "sequential fusion" – has been proposed and studied for near-barrier fusion of weekly bound neutron rich nuclei [14]. It was shown that intermediate neutron transfer with positive Q-values may significantly enhance the fusion probability at sub-barrier energies. In the process of "sequential fusion" intermediate neutrons transfer to the states with Q>0 is, in a certain sense, an "energy lift" for the two interacting nuclei – Fig. 14. The effect was found to be very large especially for fusion of weakly bound nuclei. New experiments have been proposed, in which the effect will be clearly distinguished. In this experiment the near-barrier fusion reactions ^{6}He+^{206}Pb and ^{4}He+^{208}Pb leading to the same compound nucleus ^{212}Po should be studied at the same sub-barrier center-of-mass energy (same temperature). At $E_{c.m.}$~ 15 MeV a probability for formation of Po isotopes was predicted to be 100 times larger for ^{6}He+^{206}Pb comparing with ^{4}He+^{208}Pb.

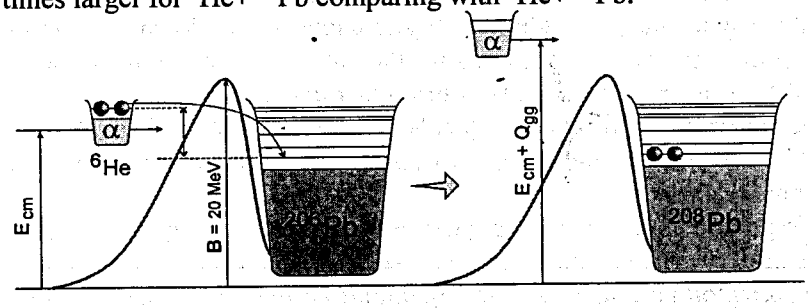

Fig. 14. Schematic picture of sequential fusion of ^{6}He with ^{208}Pb at sub-barrier energy.

Applied research

The PEM-analysis of radiation defects with a "black-white" contrast discovered in silicon irradiated by high-energy (710 MeV) Bi ions has been performed using the techniques of chemical and ionic removal of submicron layers. The chemical removal preserves the crystal structure of a pre-surface layer, while the ion dispersion, on the contrary, forms an amorphous pre-surface layer. Thus, it has been shown that along the ion track in silicon the high-energy bismuth ion causes formation of a cylindrical area with a destructive crystal lattice which is visualized in PEM as the so-called "black-white" contrast due to its deformation relaxation in the pre-surface crystal volume of silicon.

In the framework of the program for developing the technology of ion-track lithography, the peculiar features of formation in a polymeric matrix (polycarbonate) of etched submicron structures with a high-aspect ratio (40:1), when irradiating by high-energy (250 MeV) krypton ions through absorbing masks of a cylindrical form, were realized and investigated.

Possibilities of forming a porous structure in the polyimide films irradiated by ions were investigated. Structural and optical properties of track membranes on the basis of polypyromellitimide were investigated. The latter was suggested for using as radiation-proof filters of electromagnetic radiation in x-ray and ultra-violet ranges (in the structure of x-ray telescopes for research on a solar crown).

Research by the methods of atomic force microscopy on nanodimensional structural defects on a surface of monocrystals Al_2O_3, MgO and $MgAl_2O_4$ exposed to ions of krypton, xenon and bismuth with the energies in the interval of 0,6-3,5 MeV/nucleon were continued. The purpose of the work is to determine the laws of formation of structural defects on the surface of candidate materials of inert thinners (matrixes) of nuclear fuel caused by irradiation by heavy ions with the energies characteristic for fission fragments. The upper limits were determined for the values of density of ionization in a pre-surface layer of the samples from which radiation-caused changes in the surface structure of the given crystals are registered. These threshold values are 25,4 keV/nm for sapphire, 15,8 keV/nm for magnesium oxide and 15,5 keV/nm for spinel.

Experiments were carried out on determining a level of mechanical stress in ruby monocrystals in the course of irradiation by 3-7 MeV/n ions of argon, krypton and bismuth. The magnitude of the stress was determined on the R-lines shift in the spectra of luminescence generated by high-energy ions (piezo-spectroscopic effect) in the given material. It has been found that the

level of stress in the sample's layer irradiated with 710 MeV bismuth ions is not determined by a full concentration of the defects formed in elastic collisions. A basic contribution to the formation of defective structure resulting in appearing compressing mechanical stress is brought by electronic losses of the ion energy.

The influence of irradiation by fast neutrons and ions of Kr (235 MeV) and Bi (710 MeV) on the optical and electric properties 4H-SiC was investigated. In this work the methods of photoluminescence and spectroscopy of deep levels was used. Electric characteristics of Al and Cr were studied using Shottky barriers. According to experimental data the neutrons and high-energy ions cause formation identical defective centers in 4H-SiC. These results show that even at extremely high values of ionization density (34 keV/nm) the formation of a defect structure in silicon carbide monocrystals is determined by the losses of particles energy on elastic scattering.

With using of the state "Migration" a number of physical and chemical characteristics of ions In^{+3}, Cd^{+2}, Zr^{+4}, Hf^{+4} and Pu^{+6} in water solutions were determined using isotopes ^{111}In, Cd, ^{88}Zr, ^{175}Hf and ^{237}Pu.

Tests of the basic systems of accelerator DC-72 were carried out in accordance with the schedule for 2004. Magnetic measurements were carried out in full. The pumping-out of the channel of axial injection was done, tests of the water-cooling system were carried out, and projected parameters were achieved.

A draft of the heavy ion accelerator DC-60 has been developed. The accelerator should provide intense beams of accelerated ions in the energy range of 0.35-1.67 MeV/nucleon as well as ion beams from the ECR-source with the energy of 25 keV/charge. This accelerator will be used for realization of the program of fundamental and applied research. The main items are:

- track membranes and their applications.
- modification of the surface of materials.
- fundamental and applied aspects of formation and use of nuclear tracks in solids.
- ionic - implantation nanotechnology.

The project has passed the expertise at the Scientific Council of the Russian Academy of Sciences on charged particle accelerators.

Physics and heavy ion accelerator techniques

In 1998-2004, the U400 was mainly used for experiments with $_{48}Ca^{5+}$ ions for the synthesis of super heavy elements. The essential modernization of the U400 axial injection included sharp shortening of the horizontal part of

the injection canal. To increase the acceleration efficiency, the combination of line and sine bunchers has been used. The modernization gave the possibility to increase the $_{48}Ca^{+5}$ current into the injection line from 40÷60 to 80÷100 μA, Correspondingly, the average output $_{48}Ca^{+18}$ ion current was increased from 15 to 25 μA. The diagram of U-400 operation in 1997-2004 is shown in Fig. 15.

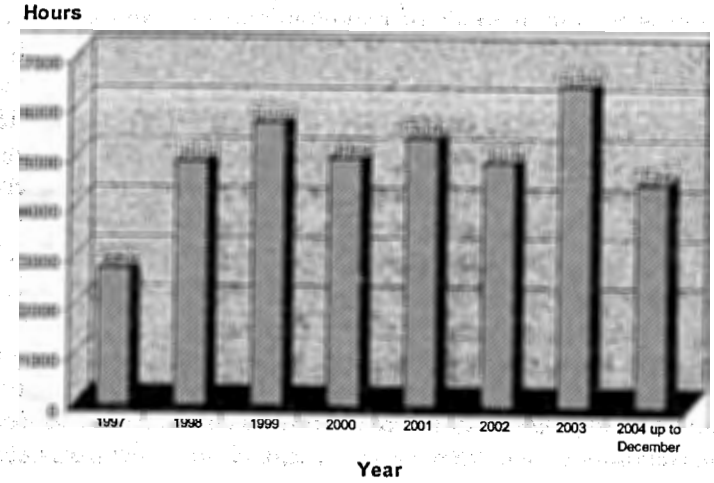

Fig. 15. The diagram of U-400 operation in 1997-2004

The modernization of the U400 has been suggested to improve the cyclotron parameters. The cyclotron parameters before (U400) and after (U400R) the modernization are shown in Table. The aims of the modernization are:

1. Decreasing the magnetic field level at the cyclotron center from the region of 1.93÷2.1 T to 0.8÷1.8 T, that allows us to decrease the electrical power of the U400R main coil power supply in four times.
2. Providing the fluent ion energy variation at factor 5 for every mass to charge ratio A/Z at accuracy of $\Delta E/E=5\cdot10^{-3}$;
3. Increasing the intensity of accelerated ions by the factor of 3.

The possibility of increasing the injection voltage from 13÷20 kV to 40÷50 kV is under study. As we estimated, the changes can give us increasing the U400R accelerating efficiency in 1.5÷2 times, it is particularly important for $_{48}Ca$ ions.

The RF system of U400R will consist of two RF generators that will excite two separated RF dee resonators. The RF resonators will be made from iron with copper coating to decrease the outgasing rate from the vacuum surface.

Cyclotron parameters before (U400) and after (U400R) modernization.

Parameters	U400	U400R
Electrical power of magnet power supply system	850 kW	200 kW
The magnetic field level in the magnet center	1.93÷2.1 T	0.8÷1.8 T
The A/Z range	5÷12	4÷12
The frequency range	5.42÷12.2 MHz	5.42÷12.2 MHz
The ultimate extraction radius	1.72 m	1.8 m
K- factor	305÷625	100÷506
Ion extraction method	Stripping foil	Stripping foil Deflector
Number of directions for ion extraction	2	2

The diagram of U-400M operation in 1998-2004 is shown in Fig. 16.

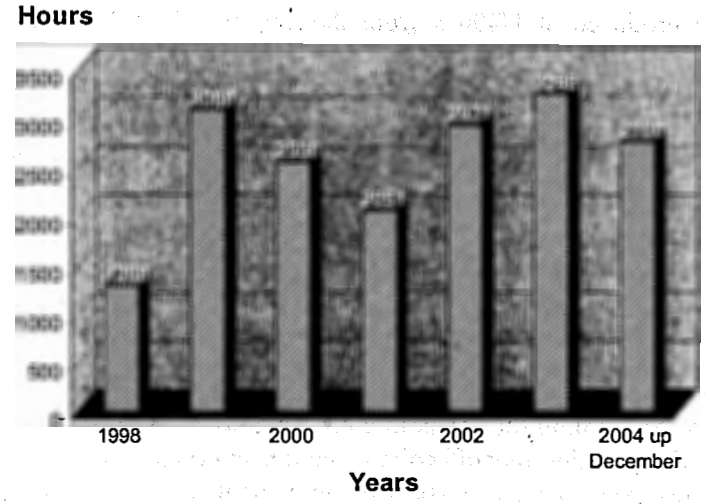

Fig. 16. The diagram of U-400M operation in 1998-2004

On the U400M cyclotron two sources of ions are installed: ECR - for production of heavy ions and high-frequency source of ions, which is used

for generation of tritium ion beam.The tritium ion beam was required for study of ^{4}H and ^{5}H resonance states in neutron transfer reactions $t+t\rightarrow{}^{5}H+p$ and $t+t\rightarrow{}^{4}H+d$. Experiments were performed at the separator ACCULINNA.

At the U400M cyclotron the tritium ions should be accelerated as molecular ions $(DT)^{+}$ from the point of view beam extraction by stripping. The required beam intensity on the liquid tritium target was about 10^{8} pps.

For production of molecular ions the RF ion source was chosen. During the operation at the test bench the ion source was optimized for production of H_2^{+} ions.

For feeding of the tritium atoms into the ion source the special gas feed system was developed in RFNC – VNIIEPh (Sarov, Russia) which provides fine regulation of gas flow and safety handling with tritium.

The hydrogen isotopes, including deuterium-tritium mixture, are chemically kept on ^{238}U. After heating of uranium the hydrogen isotopes are fed into the ion source due to diffusion through the walls of heated nickel capillary. Special attention was paid to design of the vacuum system to provide environmentally safe operation. A beam of 58-MeV tritons was delivered to the tritium target of the ACCULINNA separator.

In 2003 the first stage of the DRIBs project has been realized at the U400-U400M accelerator complex. The experiments with radioactive ^{6}He ions started in December 2004. The U400 cyclotron accelerate the secondary $^{6}He^{+}$ ions produced at U400M from the energy of 3.5 keV/amu to 5÷20 MeV/amu.

The DC-40 heavy ion cyclotron was in operation since 1985 for acceleration of ions from C to Ar with fixed energy of about 1.2 MeV/nucl. For generation of such ions the PIG ion source was used. Experiments in the field of the solid-state physics and industrial applications need to use heavy ions having the mass up to Xe. In order to get ions heavier than Ar with given energy we need a powerful ion source able to generate highly charged intense heavy ions (e.g. Kr^{15+} and Xe^{23+}). To fulfill these demands superconducting (SC) ECR ion source (Fig. 18) was built together with a new axial injection line.

The mean feature of the ECRIS is using of a small Gifford-McMahon refrigerator for cooling the solenoid coils down to 4.2 K. It maintains the superconductivity of the solenoid coils without using liquid He.

The hexapole magnet consists of permanent magnets made of NdFeB with high residual magnetization ($B_r \sim 1.3$ T). The maximum induction of the mirror magnetic field is 2 and 3 T at the beam extraction and microwave injection side respectively. The magnetic field induction at the inner surface of

the plasma chamber is equal to 1.2 T. The injected microwave frequency is 18 GHz, the maximum microwave power is 1.5 kW.

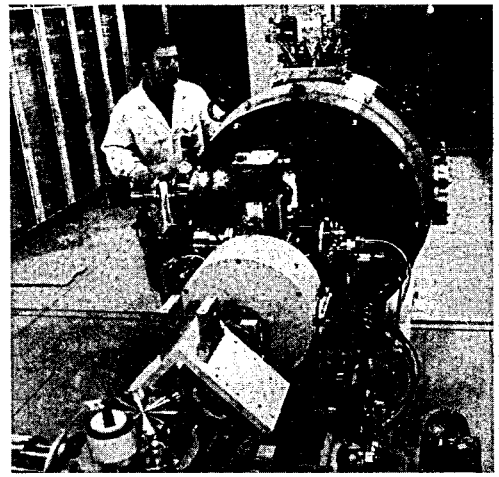

Fig. 17. Superconducting (SC) ECR ion source (ECRIS).

One of the Kr ions spectra, obtained with Sc ECRIS, is given in Fig. 18.

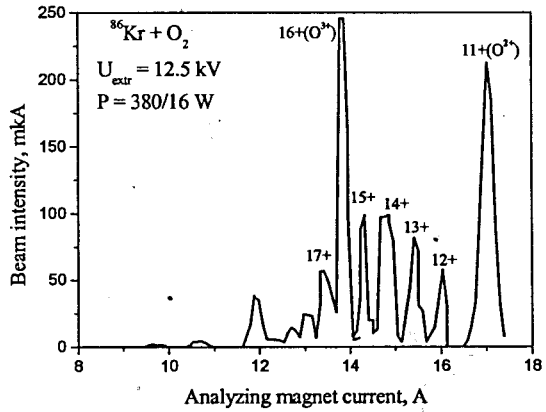

Fig. 18. The spectrum of Kr ions from SC ECRIS

At present all main cyclotron systems have been tested and given good results. Recently the cyclotron was commissioned and first accelerated beam of Kr^{15+} was extracted.

References

[1] Yu.Ts. Oganessian et al., Phys. Rev. **C69** (2004) 054607.
[2] Yu.Ts. Oganessian et al., to be published in Phys. Rev. C.
[3] Yu.Ts. Oganessian et al., Phys. Rev. **C69** (2004) 021601(R).
[4] S.N. Dmitriev et al., Preprint JINR **E12-2004-157.**
[5] M.G. Itkis et al., Nucl. Phys. **A734** (2004) 136.
[6] M. Trotta et al., Nucl. Phys . **A734** (2004) 245.
[7] V.P. Aleshin et al., to be published in Proc. of Int. Symp. "EXON-2004".
[8] L.V. Grigorenko et al., Eur. Phys. J., **A20** (2004) 419.
[9] Yu.V. Pyatkov et al., Preprint JINR **E15-2004-65.**
[10] A.A. Hassan et al., Preprint JINR **P15-2004-122.**
[11] V.Yu.Ugryumov et al., Nuclear Physics **A734** (2004) E53.
[12] V.I. Zagrebaev, Nucl. Phys., **A734** (2004) 164.
[13] Y. Aritomo et al., Progr. Theor. Phys. Suppl., **154** (2004) 449.
[14] V.I. Zagrebaev, Progr. Theor. Phys. Suppl., **154** (2004) 122.